

# Rational design of photochromic diarylbenzene with both high photoreactivity and fast thermal back reactivity

メタデータ	言語: English 出版者: Royal Society of Chemistry 公開日: 2022-10-28 キーワード (Ja): キーワード (En): 作成者: 前川, 陸人, 北川, 大地, 濱谷, 将太, 小畠, 誠也 メールアドレス: 所属: Osaka City University, Osaka City University, Osaka City University, Osaka City University
URL	<a href="https://ocu-omu.repo.nii.ac.jp/records/2020119">https://ocu-omu.repo.nii.ac.jp/records/2020119</a>

# Rational design of photochromic diarylbenzene with both high photoreactivity and fast thermal back reactivity

Rikuto Maegawa, Daichi Kitagawa, Shota Hamatani,  
Seiya Kobatake

<b>Citation</b>	New Journal of Chemistry. 45(40); 18969-18975.
<b>Issue Date</b>	2021-10-28
<b>Type</b>	Journal Article
<b>Textversion</b>	Author
<b>Relation</b>	The following article has been accepted by New Journal of chemistry. This is the accepted manuscript version. Please cite only the published version. The final, published version is available at <a href="https://doi.org/10.1039/D1NJ04047B">https://doi.org/10.1039/D1NJ04047B</a> .
<b>DOI</b>	10.1039/D1NJ04047B

Self-Archiving by Author(s)  
Placed on: Osaka City University

# Rational design of photochromic diarylbenzene with both high photoreactivity and fast thermal back reactivity

Rikuto Maegawa, Daichi Kitagawa,\* Shota Hamatani and Seiya Kobatake\*

Recently, diarylbenzenes (DABs) have been developed as a new family of T-type photochromic molecules. In this work, we newly designed and synthesized DABs for creation of the molecule having both high photoreactivity and fast thermal back reactivity. Utilizing the intramolecular CH–N hydrogen bonding and the bulky substituents at the reactive carbons resulted in the enhancement of the photoreactivity and the acceleration of the thermal back reaction rate. Furthermore, we demonstrated that the high photoreactivity resulted in much better coloration compared with that for the previously reported DAB even at the lower concentration. These results would not only provide the strategy for the molecular design but also be useful for the development of materials with less environmental load.

## Introduction

Photochromic molecules, which change their physicochemical properties in response to light, are playing active roles in the research fields of materials chemistry and life sciences.<sup>1–5</sup> As one of the representative photochromic molecules, diarylethene (DAE) derivatives have been known as a photochemically-reversible type (P-type) photochromic molecule. DAEs show  $6\pi$ -electron photocyclization and photocycloreversion reaction and have excellent properties such as high photoreactivity, rapid response, high durability, high thermal stability, and high reactivity in the solid state.<sup>6</sup> Therefore, DAEs are expected to be applied to optical memory media,<sup>7</sup> switching devices,<sup>8</sup> display materials,<sup>9</sup> nonlinear optics,<sup>10</sup> and photoactuators.<sup>11</sup> On the other hand, there are thermally-reversible type (T-type) photochromic compounds such as azobenzene, spiropyran, hexaarylbiimidazole, naphthopyran, and so on. They show the thermal back reaction from the photogenerated unstable isomer to the initial stable isomer at room temperature. Therefore, they are expected to be used for ophthalmic lenses, sensors, security inks, and so on.<sup>12–14</sup> Especially, fast T-type photochromic molecules that undergo photoisomerization only under photoirradiation and quickly return to the original state as soon as irradiation stopped are attracting much attention in application to real-time holography, super-resolution fluorescence microscopy, and so on.<sup>15–18</sup> Thus, investigation of novel photochromic molecular systems is necessary to open up new research fields and technologies.

In line with this, we have developed a diarylbenzene (DAB) molecule, 1,2-bis(2-methyl-5-phenyl-3-thienyl)tetrafluorobenzene, by introducing tetrafluorobenzene as the ethene bridge

moiety instead of perfluorocyclopentene in a representative DAE, 1,2-bis(2-methyl-5-phenyl-3-thienyl)perfluorocyclopentene.<sup>19</sup> The DAB worked as a fast T-type photochromic molecule with the half-life time ( $t_{1/2}$ ) of 130 ms at room temperature. In that case, the fast thermal back reactivity was achieved, but the photoreactivity was not so good, meaning that the quantum yield from the colorless open-ring isomer to the colored closed-ring isomer ( $\Phi_{o\rightarrow c}$ ) was about 0.3 in *n*-hexane. This is due to the equilibrium between the photoreactive anti-parallel conformation and the nonphotoreactive parallel conformation of DAB at the ground state (Fig. S1). Recently, to increase the photoreactivity, we have designed and synthesized difluorinated DAB, 1,2-bis(5-methyl-2-phenyl-4-thiazolyl)-4,5-difluorobenzene (**1a**).<sup>20</sup> DAB **1a** exhibits intramolecular CH–N hydrogen bonding between the benzene ring and the thiazole ring, resulting in the stabilization of the photoreactive anti-parallel conformation at the ground state. Therefore, the  $\Phi_{o\rightarrow c}$  in *n*-hexane was dramatically increased up to 0.91. However, replacing the fluorine atoms with hydrogen atoms slowed down the  $t_{1/2}$  of the thermal back reaction to 280 s at room temperature. To function as a fast T-type photochromic molecule, the acceleration of the thermal back reaction rate is required.

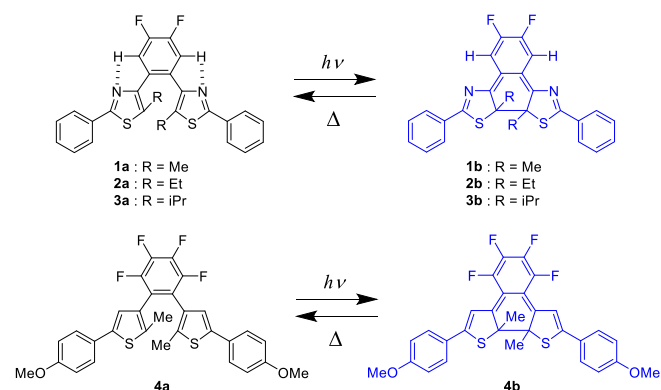
To overcome this issue, we focused on the previous studies on the thermal back reactivity of DAEs.<sup>21–25</sup> As one of the methods to control the thermal back reactivity of DAEs, the introduction of bulky alkyl substituents at the reactive carbons has been reported.<sup>26</sup> For example, the introduction of isopropyl groups at the reactive carbons instead of methyl groups led to the acceleration of the thermal back reaction rate and the  $t_{1/2}$  was sped up from 550 h to 0.33 h at 100 °C.<sup>27</sup> This is due to the destabilization of the closed-ring isomer by introducing bulky substituents at the reactive carbons. The larger energy difference between open-ring isomer to the closed-ring isomer results in an increase in the thermal back reaction.

Based on these previous findings, in this work, to attain both high photoreactivity and fast thermal back reactivity, we newly designed and synthesized DABs **2a** and **3a** having ethyl and isopropyl groups at the reactive carbons instead of methyl

Department of Applied Chemistry, Graduate School of Engineering, Osaka City University, 3-3-138 Sugimoto, Sumiyoshi-ku, Osaka 558-8585, Japan.  
E-mail: kitagawa@osaka-cu.ac.jp; kobatake@a-chem.eng.osaka-cu.ac.jp;  
Fax: +81 6 6605 2798; Tel: +81 6 6605 2798

\*Electronic Supplementary Information (ESI) available: Detailed experimental data (Figs. S1–S9 and Tables S1–S10), and movies of the photochromic behavior for **3** and **4** in *n*-hexane (Videos S1 and S2). See DOI: 10.1039/x0xx00000x

groups for **1a** (Scheme 1). The optical properties and thermal reactivities of the newly synthesized compounds were investigated and compared to those for DAB **4a** reported previously.<sup>28</sup>



Scheme 1 Diarylbenzenes investigated in this work.

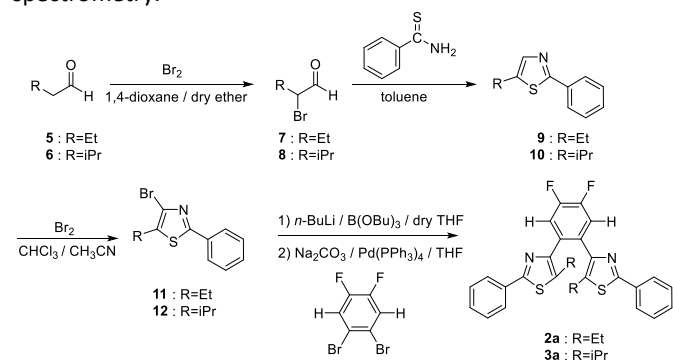
## Results and discussion

### Molecular design and synthesis

First, to predict the thermal back reactivity of DABs **2** and **3**, the activation energy ( $E_a$ ) for the thermal back reaction from the closed-ring isomer to the open-ring isomer was estimated by using DFT calculation at the M06-2X/6-31G (d) level. The calculated values of the energy for the open-ring isomer (Open), the closed-ring isomer (Closed), and the transition state (TS) are summarized in Table 1 with the data of **1**. The calculated activation energy ( $E_{a(\text{calc})}$ ) values for **2** and **3** were 85.7 and 66.8 kJ mol<sup>-1</sup>, respectively. These values are smaller than that for **1** (89.0 kJ mol<sup>-1</sup>), which indicates the faster thermal back reaction for **2** and **3** than that for **1**. The origin of the change in the  $E_{a(\text{calc})}$  values is due to the energy difference ( $\Delta E$ ) between the closed-ring isomer and open-ring isomer in the ground state. Larger  $\Delta E$  leads to lower  $E_a$  and, thus, an increase in the reactivity in the thermal back reaction. This is known as the Bell–Evans–Polanyi principle.<sup>29</sup> Furthermore, interestingly, the  $E_{a(\text{calc})}$  for **3** is very similar to that for previously reported DABs exhibiting fast T-type photochromism with the  $t_{1/2}$  of a few hundreds of ms. Thus, it was suggested that the introduction of bulky substituents at the reactive carbons is an effective method to modulate the thermal back reaction rate of DABs, as in the case of DAEs.

Based on the rational molecular design described above, **2a** and **3a** were synthesized through a cross-coupling reaction as shown in Scheme 2. The detailed procedures are described in Experimental Section. The chemical structure was confirmed by

<sup>1</sup>H and <sup>13</sup>C NMR spectroscopy and high-resolution mass spectrometry.



Scheme 2 Synthetic procedure of **2a** and **3a**.

### Photochromic Behavior in Solution

Fig. 1 shows the absorption spectral changes of **2a** and **3a** in *n*-hexane by UV light irradiation. Both **2a** and **3a** have absorption maxima ( $\lambda_{\text{max}}$ ) at 309 nm. The molar absorption coefficient at  $\lambda_{\text{max}}$  ( $\epsilon_{\text{max}}$ ) is  $2.93 \times 10^4$  and  $2.95 \times 10^4$  M<sup>-1</sup> cm<sup>-1</sup> for **2a** and **3a**, respectively. Upon irradiation with 313 nm light, the colorless solution of **2a** and **3a** turned blue, in which a visible absorption maximum was observed at 699 and 700 nm for **2b** and **3b**, respectively. The blue color of **2b** gradually disappeared after ceasing UV irradiation, while that of **3b** immediately disappeared by stopping irradiation. The absorption spectra returned to those of the initial state after disappearing the blue color. These results indicate that both **2a** and **3a** exhibit T-type photochromism and the thermal back reactivity of **3b** is higher than that of **2b**.

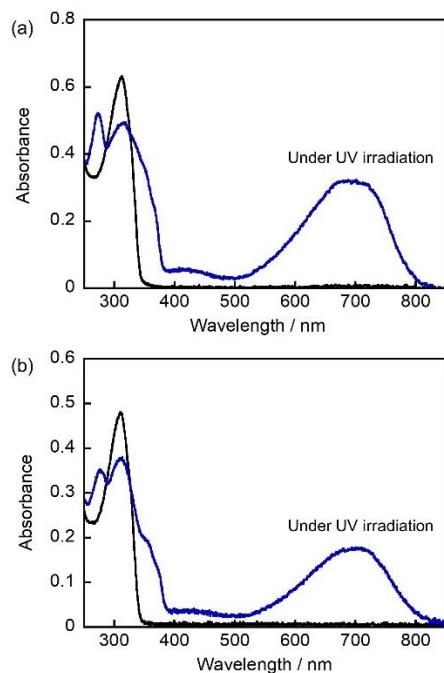
To quantitatively evaluate the thermal back reactivity, we measured the change in the absorption of **2b** and **3b** as a function of time at various temperatures (Figs. 2a and c). The absorption decay curves for **2b** and **3b** obeyed first-order kinetics and the rate constants ( $k$ ) of the thermal back reaction at various temperatures were determined (Tables S1 and S2). Figs. 2b and d show the temperature dependence of  $k$  (Arrhenius plots) for **2b** and **3b**, respectively. The experimental activation energy ( $E_{a(\text{exp})}$ ) and the frequency factor ( $A$ ) of the thermal back reaction were determined from the slope and intercept of the Arrhenius plots. The obtained values are summarized in Table 2. The  $E_{a(\text{exp})}$  values of **2b** and **3b** were 86 and 68 kJ mol<sup>-1</sup>, respectively, and show good agreement with the  $E_{a(\text{calc})}$  values estimated by DFT calculations. The  $A$  values of **2b** and **3b** were also determined to be  $2.7 \times 10^{13}$  and  $9.0 \times 10^{11}$  s<sup>-1</sup>, respectively. Using the  $E_{a(\text{calc})}$  and  $A$  values, the  $t_{1/2}$  of the thermal back reaction of **2b** and **3b** at 298 K were calculated to

Table 1. The  $E_{a(\text{calc})}$  and the  $\Delta E$  values calculated by DFT (M06-2X/6-31G (d) level of the theory).

	Energy (Open) /hartree	Energy (Closed) /hartree	Energy (TS) /hartree	$\Delta E$ /kJ mol <sup>-1 a</sup>	$E_{a(\text{calc})}$ /kJ mol <sup>-1 b</sup>
<b>1</b>	-2106.223859	-2106.186963	-2106.153083	96.9	89.0
<b>2</b>	-2184.752330	-2184.714612	-2184.681971	99.0	85.7
<b>3</b>	-2263.297505	-2263.232142	-2263.206717	171.6	66.8

<sup>a</sup>  $\Delta E = \text{Energy (Closed)} - \text{Energy (Open)}$ , <sup>b</sup>  $E_{a(\text{calc})} = \text{Energy (TS)} - \text{Energy (Closed)}$

be 30 and 0.54 s, respectively. Thus, the introduction of the bulky substituents at the reactive carbons led to the acceleration of the thermal back reaction and the fast thermal back reactivity, one of the objectives in this work, was accomplished.



**Fig. 1** Absorption spectral change of (a) **2a** and (b) **3a** in *n*-hexane: open-ring isomer (black line) and the photogenerated closed-ring isomer upon irradiation with 313 nm light (blue line).

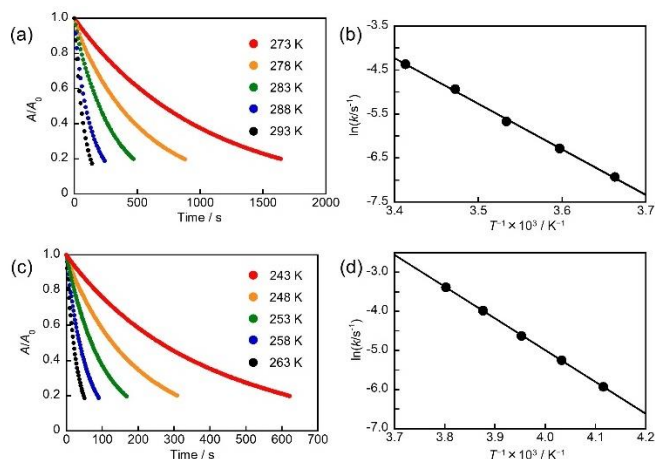


**Fig. 2** Absorbance decay curves at  $\lambda_{\max}$  for (a) **2b** and (c) **3b** in *n*-hexane at various temperatures and temperature dependence of the rate constant ( $k$ ) for the thermal back reaction of (b) **2b** and (d) **3b**.

Next, the photoreactivity from the open-ring isomer to the closed-ring isomer, the other objective in this work, was examined. We measured the absorbance change upon UV irradiation at a low temperature where the thermal back reaction can be ignored. *n*-Hexane solutions of **2a** and **3a** having the same absorbance at 313 nm were prepared. Then, irradiation with 313 nm light for 5 s and recording the absorbance were repeated multiple times. The results are shown in Fig. 3. The initial slope of the absorption changes for **2b** and **3b** was slightly smaller than that for **1b**. With an assumption that the molar extinction coefficients of the closed-ring isomers are almost equal, the  $\Phi_{o \rightarrow c}$  of **2a** and **3a** were estimated to be ca. 0.84 and 0.83, respectively, by comparing the initial slope with **1a** ( $\Phi_{o \rightarrow c} = 0.91$ ) as shown in Table S3. These values are very high compared with that for the original DAB ( $\Phi_{o \rightarrow c} = 0.3$ ), which would be due to the stabilization of the photoreactive antiparallel conformation at the ground state by the intramolecular CH-N hydrogen bonding as well as in the case of **1a**.

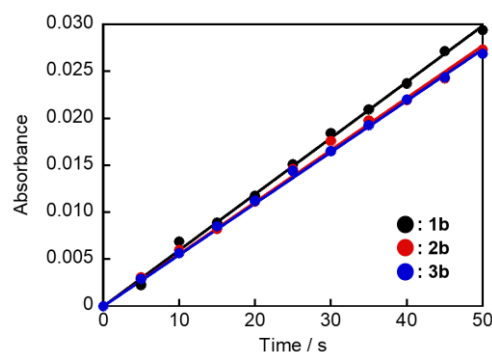


**Fig. 3** Absorbance changes of **1b** (black), **2b** (red), and **3b** (blue) at  $\lambda_{\max,203K}$  (621 nm for **1b**, 722 nm for **2b**, 718 nm for **3b**) upon irradiation with 313 nm light ( $0.89 \text{ mW cm}^{-2}$ ) at 203 K. The initial *n*-hexane solutions of **1a**, **2a**, and **3a** have the same absorbance at 313 nm ( $\text{Abs}_{313 \text{ nm}} = 0.3$ ).

To confirm the presence of the intramolecular hydrogen bonding, we measured the change in  $^1\text{H}$  NMR before and after the addition of a polar protic solvent. Fig. 4 shows the  $^1\text{H}$  NMR of **3a** in toluene- $d_8$  and mixed solvent of toluene- $d_8$  and methanol- $d_4$  (5:1). The signal corresponding to  $\text{H}_a$  atoms at the benzene ring appeared at  $\delta = 7.42\text{--}7.53$  ppm in toluene- $d_8$ , and this showed an upfield shift with the addition of methanol- $d_4$ . The signal assigned to  $\text{H}_b$  atoms at the lateral phenyl rings appeared at  $\delta = 8.09\text{--}8.17$  ppm in toluene- $d_8$ , and it also exhibited an upfield shift by the addition of methanol- $d_4$ . These results are similar to that for **1a** reported previously,<sup>20</sup> indicating the presence of intramolecular CH-N hydrogen bondings. Moreover, interestingly, the signal corresponding to  $\text{H}_c$  atoms (methine hydrogen at  $\delta = 3.32$  ppm in toluene- $d_8$ ) and

Table 2. Optical properties and Arrhenius parameters for the thermal back reaction of DABs in *n*-hexane

	$\lambda_{\max(\text{open})}/\text{nm}$	$\epsilon_{\max}/\text{M}^{-1} \text{ cm}^{-1}$	$\lambda_{\max(\text{closed})}/\text{nm}$	$E_{\text{a}(\text{exp})}/\text{kJ mol}^{-1}$	$A/\text{s}^{-1}$	$k/\text{s}^{-1}$ at 298 K	$t_{1/2}/\text{s}$ at 298 K
<b>1</b>	312	$2.80 \times 10^4$	690	88	$6.1 \times 10^{12}$	$2.5 \times 10^{-3}$	280
<b>2</b>	309	$2.93 \times 10^4$	699	86	$2.8 \times 10^{13}$	$2.3 \times 10^{-2}$	30
<b>3</b>	309	$2.95 \times 10^4$	700	68	$9.0 \times 10^{11}$	1.3	0.54

methyl hydrogens (at  $\delta = 1.06$  ppm in toluene- $d_8$ ) also exhibited an upfield shift. This result suggests that the methine hydrogen and methyl hydrogens at the isopropyl group also exhibits hydrogen bonding with the nitrogen atom of the neighboring thiazole ring, and the CH–N interactions became weak by the addition of methanol- $d_4$ . The change in  $^1\text{H}$  NMR of **2a** before and after the addition of methanol- $d_4$  was also measured as shown in Fig. S2. In this case, the upfield shift of the signals corresponding to  $\text{H}_a$ ,  $\text{H}_b$ , and methylene hydrogens ( $\text{H}_c$ ) of the ethyl groups were observed. On the other hand, the signal of methyl hydrogen atoms at the ethyl groups appeared at  $\delta = 0.99$  ppm in toluene- $d_8$  showed a downfield shift. This indicates a decrease of the ring-current effect of the neighboring thiazole ring due to the weakening of CH- $\pi$  interactions between methyl hydrogen atoms and the thiazole ring. Thus, the presence of the intramolecular CH–N interactions was confirmed by  $^1\text{H}$  NMR spectroscopic data. Moreover, from X-ray crystallographic analysis, it was revealed that the molecular structures of **2a** and **3a** in crystal were fixed in the photoreactive anti-parallel conformation as shown in Fig. S3, although all the previously reported DABs without the intramolecular CH–N interactions were crystallized in the nonphotoreactive parallel conformation. This result would also suggest the effect of the intramolecular CH–N interactions in solution.

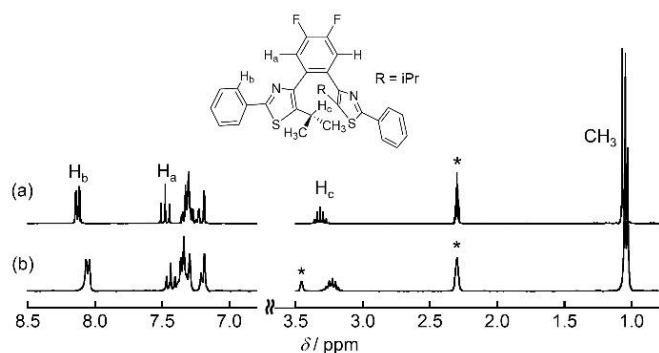


**Fig. 4**  $^1\text{H}$  NMR spectra of **3a** in (a) toluene- $d_8$  and (b) mixed solvent of toluene- $d_8$  and methanol- $d_4$  (5:1). The signals assigned to toluene and methanol was marked by asterisk.

Finally, the photochromic behavior of **3** was compared with that of previously reported **4** having the  $t_{1/2}$  of 510 ms at 298 K. The  $t_{1/2}$  for **4** is very similar to **3** (540 ms at 298 K), but the photoreactivity is not so good ( $\Phi_{o\rightarrow c} = 0.34$ ) compared with that for **3** as shown in Fig. S4. This is due to that DAB **4** does not have the intramolecular hydrogen bonding to stabilize the photoreactive antiparallel conformation at the ground state. Therefore, to see the usefulness of the difference in the photoreactivity between **3** and **4**, we investigated the photochromic behavior in solution at room temperature. The *n*-hexane solutions containing **3a** and **4a** were prepared, in which the absorbance at 313 nm was adjusted to be the same. The concentration of **3a** and **4a** in the solutions was  $5.28 \times 10^{-5}$  and  $7.43 \times 10^{-5}$  M, respectively. Fig. 5 and Videos S1 and S2 show the coloration upon UV irradiation and the decoloration after ceasing UV irradiation in *n*-hexane for **3** and **4**. As can be seen, in spite of the lower concentration of **3**, the coloration of **3a**

upon UV irradiation is much better than that of **4a**. The enhancement of the coloration is thanks to the improvement in the photoreactivity. Most of molecules of **3a** are fixed in the photoreactive anti-parallel conformation even in solution, resulting in the very good coloration. On the other hand, molecules of **4** are in the equilibrium between the photoreactive anti-parallel conformation and the nonphotoreactive parallel conformation, resulting in the poor coloration. Thus, high photoreactivity enables coloring with a smaller amount and would be useful for the development of materials with less environmental load.

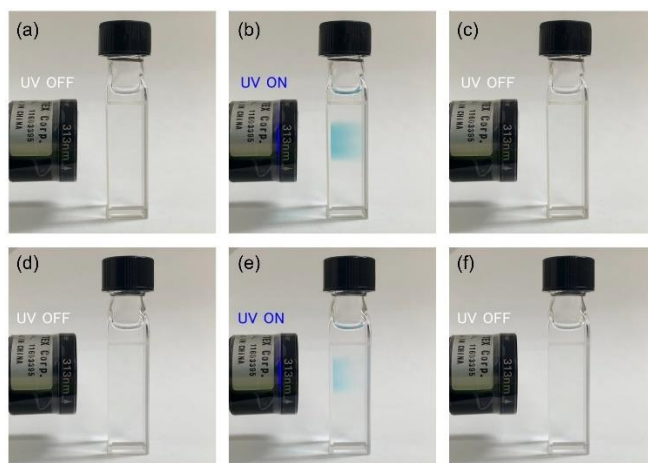


**Fig. 5** Photochromic behavior of **3** and **4** in *n*-hexane at room temperature. (a, d) Before UV irradiation, (b, e) under UV irradiation, and (c, f) 2 s after ceasing UV irradiation. The initial *n*-hexane solutions of **3a** and **4a** have the same absorbance at 313 nm ( $A_{313\text{ nm}} = 1.5$ ). The intensity of the UV light (313 nm) was  $4.3 \text{ mW cm}^{-2}$ .

## Experimental

### General

Solvents used were of spectroscopic grade and purified by distillation before use. Recycle preparative high-performance liquid chromatography (HPLC) for purification of compounds were performed by a JASCO UV-4075/PU-4086 HPLC system equipped with two JAIGEL-2HR columns using chloroform as the eluent.  $^1\text{H}$  NMR (300 MHz) and  $^{13}\text{C}$  NMR (75 MHz) spectra were recorded on a Bruker AV-300N spectrometer with tetramethylsilane (TMS) as the internal standard. High-resolution mass spectra (HRMS) were obtained on a JEOL AccTOF LC mass spectrometer. Quantum chemical calculations of open-ring isomers (Open), closed-ring isomers (Closed), and transition states (TS) were performed by the same procedures reported previously using Gaussian16 Rev.C.01 program package.<sup>30-32</sup> Single crystal X-ray crystallographic analysis was carried out using a Rigaku AFC/Mercury CCD diffractometer with  $\text{MoK}\alpha$  radiation ( $\lambda = 0.71073 \text{ \AA}$ ) monochromated by graphite. The crystal structures were solved by a direct method using SIR92 and refined by the full matrix least-squares method on  $F^2$  with anisotropic displacement parameters for non-hydrogen atoms using SHELXL-2014.

### Absorption Spectroscopy

UV-Vis absorption spectra in *n*-hexane were measured using a JASCO V-560 absorption spectrometer or an Ocean Optics FLAME-S multichannel analyzer. Photoirradiation was carried out using a 300 W xenon lamp (Asahi Spectra MAX-301) or a 200 W mercury-xenon lamp (Moritex MSU-6) as a light source. Monochromatic light (313 nm light) was obtained by passing light through a band-pass filter. Photochemical reaction at low temperature was carried out as follows. Photocyclization reaction was followed by absorption spectra. The samples were not degassed. The optical quartz cell containing samples was placed in a cryostat for spectroscopy (UNISOKU CoolSpeK UV/CD) during the photochemical reaction.

## Materials

Chemicals used for synthesis were commercially available and used without further purification. **1a** and **4a** were synthesized by the method reported previously.<sup>26,28</sup> **2a** and **3a** were synthesized as shown in Scheme 2.

**5-Ethyl-2-phenylthiazole (9)**. Thiobenzamide (3.6 g, 26 mmol) was dissolved in toluene (50 mL) at 80 °C. 2-Bromobutanal (**7**) (4.0 g, 26 mmol) dissolved in a small amount of toluene was added dropwise into the solution, and the mixture was refluxed at 130 °C for 3 h. Toluene was evaporated, and reaction mixture was neutralized by NaHCO<sub>3</sub> aqueous solution, extracted with ethyl acetate, washed with brine, dried over MgSO<sub>4</sub>, filtered, and concentrated in vacuo. The crude product was purified by column chromatography on silica gel *n*-hexane and ethyl acetate (9:1) as the eluent to give 2.2 g of **9** in 43% yield. <sup>1</sup>H NMR (300 MHz, CDCl<sub>3</sub>, TMS)  $\delta$  = 1.36 (t, *J* = 7.6 Hz, 3H, CH<sub>3</sub>), 2.89 (qd, *J* = 7.6 and 1.0 Hz, 2H, CH<sub>2</sub>), 7.38–7.45 (m, 3H, Aromatic), 7.53 (t, *J* = 1.0 Hz, 1H, thienyl), 7.88–7.92 (m, 2H, Aromatic). <sup>13</sup>C NMR (75 MHz, CDCl<sub>3</sub>)  $\delta$  = 16.2, 20.8, 126.3, 129.0, 129.7, 134.2, 139.9, 141.8, 166.5. HRMS (ESI-TOF) *m/z* = 190.0686 (MH<sup>+</sup>). Calc for C<sub>11</sub>H<sub>12</sub>NS<sup>+</sup> = 190.0685.

**4-Bromo-5-ethyl-2-phenylthiazole (11)**. 5-Ethyl-2-phenylthiazole (**9**) (2.2 g, 11 mmol) was dissolved in mixed solution of CH<sub>3</sub>Cl (40 mL) and CH<sub>2</sub>CN (40 mL). Bromine (2.0 mL, 39 mmol) was added dropwise into the stirring solution at 0 °C, and the mixture was stirred overnight at room temperature. The reaction mixture was neutralized by NaOH aqueous solution, extracted with chloroform, washed with brine, dried over MgSO<sub>4</sub>, filtered, and concentrated in vacuo. The crude product was purified by column chromatography on silica gel *n*-hexane and ethyl acetate (9:1) as the eluent to give 920 mg of **11** in 30% yield. <sup>1</sup>H NMR (300 MHz, CDCl<sub>3</sub>, TMS)  $\delta$  = 1.31 (t, *J* = 7.6 Hz, 3H, CH<sub>3</sub>), 2.83 (q, *J* = 7.6 Hz, 2H, CH<sub>2</sub>), 7.39–7.43 (m, 3H, Aromatic), 7.85–7.91 (m, 2H, Aromatic). <sup>13</sup>C NMR (75 MHz, CDCl<sub>3</sub>)  $\delta$  = 15.4, 21.6, 123.9, 126.1, 129.0, 130.3, 133.1, 136.1, 165.5. HRMS (ESI-TOF) *m/z* = 267.9790 (MH<sup>+</sup>). Calc for C<sub>11</sub>H<sub>11</sub>BrNS<sup>+</sup> = 267.9790.

**1,2-Bis(5-ethyl-2-phenyl-4-thiazolyl)-4,5-difluorobenzene (2a)**. 4-Bromo-5-ethyl-2-phenylthiazole (**11**) (750 mg, 2.8 mmol) was dissolved in anhydrous THF (15 mL) under argon atmosphere. 1.6 M *n*-BuLi hexane solution (2.0 mL, 3.2 mmol) was slowly added dropwise to the solution at –78 °C, and the mixture was stirred for 30 min. Tri-*n*-butyl borate (0.83 mL, 3.1 mmol) was slowly added to the solution at the temperature,

and the mixture was stirred for 40 min. An adequate amount of distilled water was added to the mixture to quench the reaction. 1,2-Dibromo-4,5-difluorobenzene (340 mg, 1.3 mmol), tetrakis(triphenylphosphine)palladium(0) (50 mg, 0.043 mmol), and 20wt% Na<sub>2</sub>CO<sub>3</sub> aqueous solution (10 mL) were added, and the mixture was refluxed for 34 h. The reaction mixture was neutralized by HCl aqueous solution, extracted with ether, washed with brine, dried over MgSO<sub>4</sub>, filtered, and concentrated in vacuo. The crude product was purified by column chromatography on silica gel using *n*-hexane and ethyl acetate (9:1) as the eluent and recycle HPLC using chloroform as the eluent to give 120 mg of **2a** in 20% yield based on 1,2-dibromo-4,5-difluorobenzene. **2a**: <sup>1</sup>H NMR (300 MHz, CDCl<sub>3</sub>, TMS)  $\delta$  = 0.99 (t, *J* = 7.5 Hz, 6H, CH<sub>3</sub>), 2.48 (q, *J* = 7.5 Hz, 4H, CH<sub>2</sub>), 7.35–7.45 (m, 8H, Aromatic), 7.83–7.87 (m, 4H, Aromatic). <sup>13</sup>C NMR (75 MHz, CDCl<sub>3</sub>)  $\delta$  = 16.4, 20.7, 119.8 (dd, <sup>2</sup>*J*<sub>CF</sub> = 11.0 Hz, <sup>3</sup>*J*<sub>CF</sub> = 7.7 Hz), 126.4, 129.0, 129.8, 132.1 (dd, <sup>3</sup>*J*<sub>CF</sub> = <sup>4</sup>*J*<sub>CF</sub> = 5.0 Hz), 133.9, 138.8, 149.0, 150.0 (dd, <sup>1</sup>*J*<sub>CF</sub> = 252.5 Hz, <sup>2</sup>*J*<sub>CF</sub> = 14.9 Hz), 164.3. HRMS (ESI-TOF) *m/z* = 489.1256 (MH<sup>+</sup>). Calc for C<sub>28</sub>H<sub>23</sub>F<sub>2</sub>N<sub>2</sub>S<sub>2</sub><sup>+</sup> = 489.1265.

**4-Bromo-5-isopropyl-2-phenylthiazole (12)**. 5-Isopropyl-2-phenylthiazole (**10**) (2.0 g, 10 mmol) was dissolved in CH<sub>2</sub>Cl<sub>2</sub> (40 mL). *N*-Bromosuccinimide (1.8 g, 10 mmol) was added to the solution at room temperature, and the mixture was stirred overnight. The reaction mixture was neutralized by NaHCO<sub>3</sub> aqueous solution, extracted with CH<sub>2</sub>Cl<sub>2</sub>, washed with brine, dried over MgSO<sub>4</sub>, filtered, and concentrated in vacuo. The crude product was purified by column chromatography on silica gel *n*-hexane and ethyl acetate (9:1) as the eluent to give 1.4 g of **12** in 50% yield. <sup>1</sup>H NMR (300 MHz, CDCl<sub>3</sub>, TMS)  $\delta$  = 1.34 (d, *J* = 6.8 Hz, 12H, CH), 3.33 (sep, *J* = 6.8 Hz, 2H, CH), 7.40–7.44 (m, 6H, Aromatic), 7.87–7.90 (m, 4H, Aromatic). <sup>13</sup>C NMR (75 MHz, CDCl<sub>3</sub>)  $\delta$  = 24.3, 29.0, 122.8, 126.1, 129.1, 130.3, 133.2, 141.9, 165.3. HRMS (ESI-TOF) *m/z* = 281.9944 (MH<sup>+</sup>). Calc for C<sub>12</sub>H<sub>13</sub>BrNS<sup>+</sup> = 281.9947.

**1,2-Bis(5-isopropyl-2-phenyl-4-thiazolyl)-4,5-difluorobenzene (3a)**. 4-Bromo-5-isopropyl-2-phenylthiazole (**12**) (1.4 g, 4.9 mmol) was dissolved in anhydrous THF (20 mL) under argon atmosphere. 1.6 M *n*-BuLi hexane solution (3.3 mL, 5.3 mmol) was slowly added dropwise to the solution at –78 °C, and the mixture was stirred for 30 min. Tri-*n*-butyl borate (1.4 mL, 5.2 mmol) was slowly added to the solution at the temperature, and the mixture was stirred for 40 min. An adequate amount of distilled water was added to the mixture to quench the reaction. 1,2-Dibromo-4,5-difluorobenzene (630 mg, 2.3 mmol), tetrakis(triphenylphosphine)palladium(0) (150 mg, 0.13 mmol), and 20wt% Na<sub>2</sub>CO<sub>3</sub> aqueous solution (10 mL) were added, and the mixture was refluxed for 22 h. The reaction mixture was neutralized by HCl aqueous solution, extracted with ether, washed with brine, dried over MgSO<sub>4</sub>, filtered, and concentrated in vacuo. The crude product was purified by column chromatography on silica gel using *n*-hexane and ethyl acetate (9:1) as the eluent and recycle HPLC using chloroform as the eluent to give 180 mg of **3a** in 15% yield based on 1,2-dibromo-4,5-difluorobenzene. **3a**: <sup>1</sup>H NMR (300 MHz, CDCl<sub>3</sub>, TMS)  $\delta$  = 0.94 (d, *J* = 6.8 Hz, 12H, CH<sub>3</sub>), 3.01 (sep, *J* = 6.8 Hz, 2H, CH), 7.36–7.42 (m, 8H, Aromatic), 7.84–7.87 (m, 4H, Aromatic).

$^{13}\text{C}$  NMR (75 MHz,  $\text{CDCl}_3$ )  $\delta$  = 25.6, 28.0, 119.9 (dd,  $^2J_{\text{CF}}$  = 11.0 Hz,  $^3J_{\text{CF}}$  = 7.7 Hz), 126.4, 129.0, 129.9, 132.2 (dd,  $^3J_{\text{CF}}$  =  $^4J_{\text{CF}}$  = 5.0 Hz), 133.9, 145.2, 147.9, 150.2 (dd,  $^1J_{\text{CF}}$  = 252.3 Hz,  $^2J_{\text{CF}}$  = 14.0 Hz), 164.4. HRMS (ESI-TOF)  $m/z$  = 539.1414 ( $\text{MNa}^+$ ). Calc for  $\text{C}_{30}\text{H}_{26}\text{F}_2\text{N}_2\text{NaS}_2^+$  = 539.1398.

## Conclusions

In this study, we newly designed and synthesized DABs **2a** and **3a** for realizing the molecule with both high photoreactivity and fast thermal back reactivity. The bulkiness of the substituents at the reactive carbons accelerated the thermal back reaction rate and the  $t_{1/2}$  of **3b** was 540 ms. This can be categorized into the fast T-type photochromism with the  $t_{1/2}$  ranging from ns to ms. Furthermore, the photocyclization quantum yields of **2a** and **3a** were estimated to be 0.84 and 0.83, which is very high compared with the typical diarylbenzenes reported previously. This is thanks to the stabilization of the photoreactive anti-parallel conformation by introducing the intramolecular CH-N hydrogen bonding. Thus, both high photoreactivity and fast thermal back reactivity was accomplished for DAB **3**. Furthermore, we demonstrated the usefulness of DAB **3** comparing the photochromic behavior with previously reported DAB **4**. The high photoreactivity resulted in the good coloration, although the  $t_{1/2}$  of **3** and **4** is very similar. These results would not only provide the strategy for the molecular design but also be useful for the development of materials with less environmental load.

## Author Contributions

**Rikuto Maegawa**: Investigation, Formal analysis, Visualization, Writing – original draft; **Daichi Kitagawa**: Conceptualization, Methodology, Formal analysis, Project administration, Resources, Supervision, Writing – original draft, Writing – review & editing; **Shota Hamatani**: Investigation, Formal analysis, Visualization, Writing – original draft; **Seiya Kobatake**: Resources, Project administration, Supervision, Writing – review & editing.

## Conflicts of interest

There are no conflicts to declare.

## Acknowledgements

This work was partly supported by JSPS KAKENHI Grant Numbers 21K14603 for D.K. and 21H02016 for S.K.

## Notes and references

1. A. Kometani, Y. Inagaki, K. Mutoh and J. Abe, *J. Am. Chem. Soc.*, 2020, **142**, 7995-8005.
2. K. Klaue, Y. Garmshausen and S. Hecht, *Angew. Chem. Int. Ed.*, 2018, **57**, 1414-1417.
3. V. A. Barachevsky, *J. Photochem. Photobiol. A: Chem.*, 2018, **354**, 61-69.
4. T. Nakashima, K. Tsuchie, R. Kanazawa, R. Li, S. Iijima, O. Galangau, H. Nakagawa, K. Mutoh, Y. Kobayashi, J. Abe and T. Kawai, *J. Am. Chem. Soc.*, 2015, **137**, 7023-7026.
5. R. Nishimura, A. Fujimoto, N. Yasuda, M. Morimoto, T. Nagasaka, H. Sotome, S. Ito, H. Miyasaka, S. Yokojima, S. Nakamura, B. L. Feringa and K. Uchida, *Angew. Chem. Int. Ed.*, 2019, **58**, 13308-13312.
6. M. Irie, T. Fukaminato, K. Matsuda and S. Kobatake, *Chem. Rev.*, 2014, **114**, 12174-12277.
7. M. Irie and K. Matsuda, in *Electron Transfer in Chemistry*, ed. V. Balzani, Wiley-VCH, Weinheim, 2001, vol. 5, pp. 215-242.
8. M. Irie, in *Molecular Switchings*, ed. B. L. Feringa, Wiley-VCH, Weinheim, 2001, pp. 37-62.
9. C. Bechinger, S. Ferrere, A. Zaban, J. Sprague and B. A. Gregg, *Nature*, 1996, **383**, 608-610.
10. J. A. Delaire and K. Nakatani, *Chem. Rev.*, 2000, **100**, 1817-1846.
11. S. Kobatake, S. Takami, H. Muto, T. Ishikawa and M. Irie, *Nature*, 2007, **446**, 778-781.
12. Y. Inagaki, Y. Kobayashi, K. Mutoh and J. Abe, *J. Am. Chem. Soc.*, 2017, **139**, 13429-13441.
13. Y. Kobayashi, K. Mutoh and J. Abe, *J. Photochem. Photobiol. C: Photochem. Rev.*, 2018, **34**, 2-28.
14. I. S. Park, Y. S. Jung, K. J. Lee and J. M. Kim, *Chem. Commun.*, 2010, **46**, 2859-2861.
15. N. Ishii, T. Kato and J. Abe, *Sci. Rep.*, 2012, **2**, 819.
16. J. Cusido, S. S. Ragab, E. R. Thapaliya, S. Swaminathan, J. Garcia-Amorós, M. J. Roberti, B. Araoz, M. M. A. Mazza, S. Yamazaki, A. M. Scott, F. M. Raymo and M. L. Bossi, *J. Phys. Chem. C*, 2016, **120**, 12860-12870.
17. E. Deniz, M. Tomasulo, J. Cusido, I. Yildiz, M. Petriella, M. L. Bossi, S. Sortino and F. M. Raymo, *J. Phys. Chem. C*, 2012, **116**, 6058-6068.
18. Y. Kobayashi and J. Abe, *Adv. Opt. Mater.*, 2016, **4**, 1354-1357.
19. D. Kitagawa, T. Nakahama, Y. Nakai and S. Kobatake, *J. Mater. Chem. C*, 2019, **7**, 2865-2870.
20. S. Hamatani, D. Kitagawa and S. Kobatake, *J. Phys. Chem. C*, 2021, **125**, 4588-4594.
21. K. Inaba, R. Iwai, M. Morimoto and M. Irie, *Photochem. Photobiol. Sci.*, 2019, **18**, 2136-2141.
22. S. Kawai, T. Nakashima, K. Atsumi, T. Sakai, M. Harigai, Y. Imamoto, H. Kamikubo, M. Kataoka and T. Kawai, *Chem. Mater.*, 2007, **19**, 3479-3483.
23. Y. H. Yang, Y. S. Xie, Q. Zhang, K. Nakatani, H. Tian and W. H. Zhu, *Chem. Eur. J.*, 2012, **18**, 11685-11694.
24. K. Uchida, T. Matsuoka, K. Sayo, M. Iwamoto, S. Hayashi and M. Irie, *Chem. Lett.*, 1999, 835-836.
25. S. Nakamura and M. Irie, *J. Org. Chem.*, 1988, **53**, 6136-6138.
26. D. Kitagawa and S. Kobatake, *Chem. Rec.*, 2016, **16**, 2005-2015.
27. S. Kobatake, K. Uchida, E. Tsuchida and M. Irie, *Chem. Lett.*, 2000, 1340-1341.
28. T. Nakahama, D. Kitagawa and S. Kobatake, *J. Phys. Chem. C*, 2019, **123**, 31212-31218.
29. F. A. Carey and R. J. Sundberg, *Advanced Organic Chemistry: Part A: Structure and Mechanisms*, Springer Science & Business Media, 2007.
30. D. Kitagawa, N. Takahashi, T. Nakahama and S. Kobatake, *Photochem. Photobiol. Sci.*, 2020, **19**, 644-653.
31. S. Hamatani, D. Kitagawa, T. Nakahama and S. Kobatake, *Tetrahedron Lett.*, 2020, **61**, 151968.
32. M. J. Frisch, G. W. Trucks, H. B. Schlegel, G. E. Scuseria, M. A. Robb, J. R. Cheeseman, G. Scalmani, V. Barone, G. A. Petersson, H. Nakatsuji, X. Li, M. Caricato, A. V. Marenich, J. Bloino, B. G.

Janesko, R. Gomperts, B. Mennucci, H. P. Hratchian, J. V. Ortiz, A. F. Izmaylov, J. L. Sonnenberg, D. Williams-Young, F. Ding, F. Lipparini, F. Egidi, J. Goings, B. Peng, A. Petrone, T. Henderson, D. Ranasinghe, V. G. Zakrzewski, J. Gao, N. Rega, G. Zheng, W. Liang, M. Hada, M. Ehara, K. Toyota, R. Fukuda, J. Hasegawa, M. Ishida, T. Nakajima, Y. Honda, O. Kitao, H. Nakai, T. Vreven, K. Throssell, J. A. Montgomery, Jr., J. E. Peralta, F. Ogliaro, M. J. Bearpark, J. J. Heyd, E. N. Brothers, K. N. Kudin, V. N. Staroverov, T. A. Keith, R. Kobayashi, J. Normand, K. Raghavachari, A. P. Rendell, J. C. Burant, S. S. Iyengar, J. Tomasi, M. Cossi, J. M. Millam, M. Klene, C. Adamo, R. Cammi, J. W. Ochterski, R. L. Martin, K. Morokuma, O. Farkas, J. B. Foresman, and D. J. Fox, Gaussian 16 (Gaussian, Inc., Wallingford CT, 2019).